Control of Calcium Carbonate Polymorphism and Morphology through Biomimetic Mineralization by means of Nanotechnology

Kazuhiko Ichikawa,* Noriyuki Shimomura, Masanori Yamada, and Naoki Ohkubo[a]

Abstract: In vitro biomimetic mineralization by means of nanotechnology allows the formation of calcium carbonate polymorphs at low temperatures ($<25\,^{\circ}C$) under a CO_2 atmosphere of 500 – 1500 ppm . A two-dimensional zinc-ion ordered array (zinc array), which acts as an active-site mimic of carbonic anhydrase, has been prepared by immersing the self-organized monolayer of 3-(2-imidazolin-1-y)propyltriethosilane on mica (ImSi substrate) into aqueous zinc solution. The zinc array mounted on the ImSi substrate catalyzed the conversion from CO_2 to HCO_3^-, and accelerated the formation of calcium carbonate. In situ X-ray diffraction data of the formed calcium carbonate on the poly(L-aspartate)-coated chitin substrate (pAsp substrate), with calcium ion-recognition sites, demonstrated that the interaction between the zinc array and pAsp substrates formed both vaterite and calcite at low temperature (15 °C) and mainly vaterite at 25 °C; this interaction also controlled the morphology of calcium carbonate formed on pAsp substrate.

Keywords: biomimetic mineralization · calcium carbonate · carbonic anhydrase · nanotechnology · polymorphism

Introduction

The marine invertebrate animals of mollusk, coral, and forminifera undergo elaborate in-vivo biomineralization by using carbon dioxide dissolved from the atmosphere into seawater. The polymorphism of calcium carbonate, which consists of aragonite, vaterite, and calcite in mollusk shells, is controlled by organic matrix proteins.[1, 2] The nacrein extracted from the nacreous shell layers has carbonic anhydrase (CA) as the main CO_2 hydration enzyme, the active site of which is zinc-bound H_2O/OH^-.[3] The in-vitro mineralization has been tried using the macromolecules extracted from the nacreous shell layers.[4]

The effect of Asp/Glu-rich macromolecules, which can recognize and bind to calcium ions, on the control over calcium carbonate polymorphism has been revealed scanning electron micrographs, optical microscopy images, and powder X-ray diffraction patterns.[1, 4a, 5, 6]The role of the CA-active sites in biomineralization or biomimetic mineralization has not yet been reported, except for a preliminary study on the skeleton formation in coral.[7]

Our research target is to use in vitro biomimetic mineralization by means of nanotechniques to form the polymorphs of calcium carbonate in aqueous solution at low temperatures ($\leq 25\,^{\circ}C$) under atmospheric pressure. The zinc model compounds that act as CA active-site mimics were designed and prepared by using biomimetic ligands.[8] In this work the two-dimensional-ordered array of zinc ions that coordinate water molecules as mimetic CA-active sites have, for the first time, been prepared at a surface; the self-organized monolayer of 3-(2-imidazolin-1-yl)propyltriethosilane (ImSi) on mica substrate (zinc-array substrate, Scheme 1). The poly(L-aspartate)

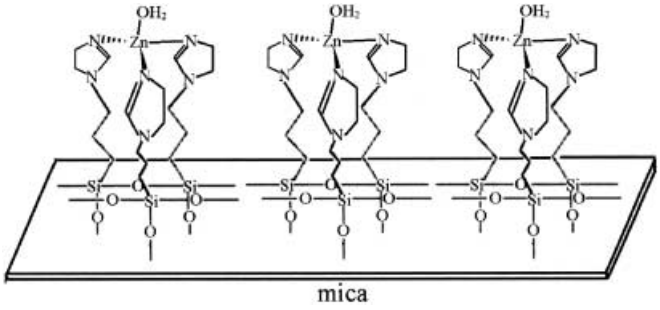

Scheme 1. A proposed geometry of zinc-coordinated ImSi adsorbed onto a mica substrate.

(pAsp-assisted) calcification, with the pAsp-coated chitin substrate providing the calcium binding sites, may be realized from the reaction of Ca^{2+} with HCO_3^-, formed by the zinc array accelerated CO_2-hydration reaction. To our knowledge, this is the first time biomimetic mineralization has been carried out by preparing a mimic for the CA active site from a zinc-array substrate by using nanotechniques.

[a] Prof. Dr. K. Ichikawa, N. Shimomura, Dr. M. Yamada, N. Ohkubo
Graduate School of Environmental Earth Science
Hokkaido University Sapporo, 060-0810 (Japan)
Fax: (+81) 11-706-7306
E-mail: ichikawa@ees.hokudai.ac.jp

 DOI: 10.1002/chem.200204534

Results and Discussion

Characterization of ImSi substrate: The atomic force microscopy (AFM) image of the mica surface covered with ImSi is shown in Figure 1. The ImSi substrate has a square hole, the surface of which gave the atomic resolution AFM image of the muscovite mica *a-b* lattice (Figure 1b);[9] the depth of about 0.9 nm was in good agreement with each ImSi molecular length (Figure 1c). Thus, the adsorbed ImSi molecules on mica surface have been characterized as their self-organized monolayer (ImSi substrate); a possible mechanism for ImSi molecules to anchor to the mica surface is described in the literature.[9]

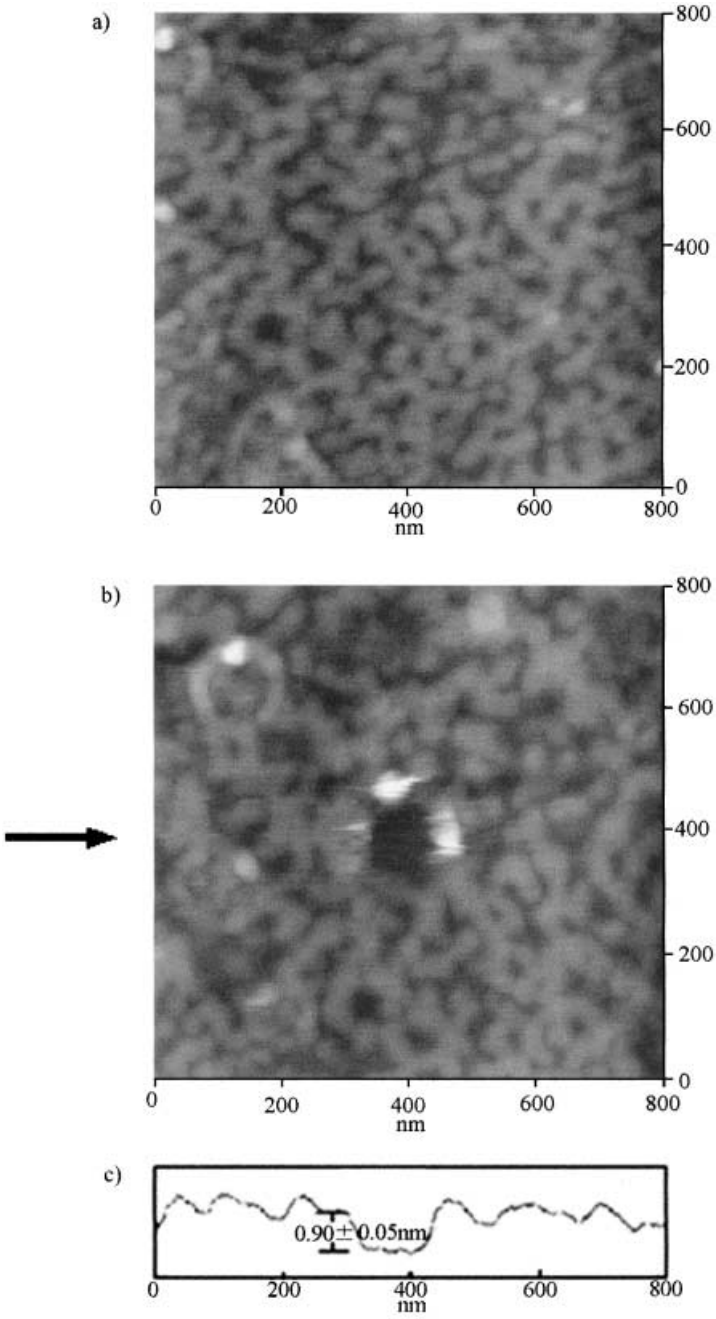

Figure 1. a) An AFM image of the self-organized ImSi monolayer over mica surface (ImSi substrate). b) The AFM image of the self-organized ImSi monolayer observed in air over ImSi sustrate surface after digging a hole ($100 \times 100\ nm^2$) by adding the scanning force 100 nN into AFM cantilever. c) Cross-section profile along the direction of the arrow in b).

Characterization of the chitin substrate and the pAsp-coated chitin substrate: The chitin coated on a strip of glass (chitin substrate) was identified from reflectance spectra recorded by using Fourier transform infrared spectroscopy (FTS-60A/896, BIORADORA). The observed IR bands around 1500, 1650, and 3250 cm^{-1} were assigned to the N–H deforming, >C=O stretching, and >N–H stretching vibrations, respectively, in each amide bond; one of the other observed bands around 2950 cm^{-1} was assigned to the methyl group C–H stretching vibration. Thus, it was confirmed that the glass substrate surface was coated by chitin. The AFM images of the chitin substrate in aqueous 5×10^{-5} or 5×10^{-4} % wt pAsp solution showed that the formed islands have a height of about 1.6 nm (Figure 2), and their diameters increased with increasing pAsp concentration (ca. 300 and 400 nm in diameter at 5×10^{-5} and 5×10^{-4} % wt pAsp, respectively). The dynamic

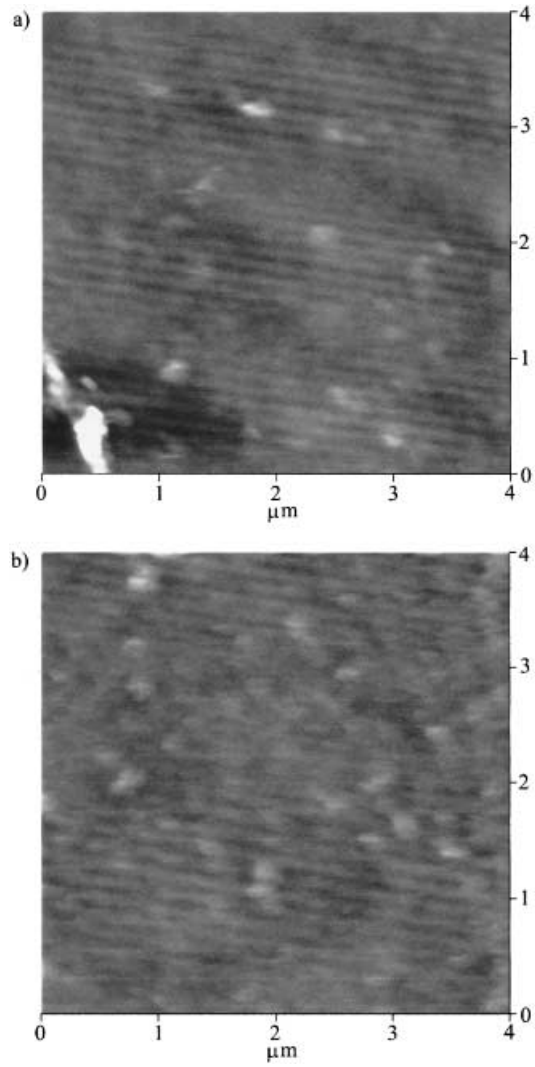

Figure 2. The AFM images of the chitin substrates immersed into aqueous a) 5×10^{-5} and b) 5×10^{-4} % wt pAsp solutions.

stationary state may be established between the pAsp dissolved in aqueous solution and the adsorbed pAsp on chitin substrate (pAsp-coated chitin substrate).

Two-dimensional zinc-ordered array and CA-like activity: The zinc-array substrate was prepared by immersing the ImSi substrate into aqueous 5 mM $Zn(NO_3)_2 \cdot 6H_2O$ solution. The force-displacement curves between the ImSi substrate and the usual Si_3N_4 cantilever were measured in pure water or aqueous 5 mM $Zn(NO_3)_2 \cdot 6H_2O$ solution by using the AFM technique, as shown in Figure 3a and b. The adhesion forces in the presence and absence of zinc ions were determined to be 1.80 and 1.75 nN, respectively. The adhesion force results from the intermolecular force between the cantilever surface and the ImSi-substrate surface. It was impossible to observe the adhesion force difference between the presence and absence of zinc ions on ImSi substrate, and to discriminate the zinc ions when used on a usual Si_3N_4 cantilever. The force-displacement curves were measured using the ImSi-modified Si_3N_4 cantilever (Scheme 2), that is, chemical force microscopy (CFM) was measured for each ImSi substrate covered with pure water or aqueous 5 mM $Zn(NO_3)_2 \cdot 6H_2O$ solution, as shown in Figure 3c and d. The adhesion forces for the zinc-array and ImSi substrates were determined to be 7.1 and 2.3 nN, respectively. Therefore, the ImSi-modified Si_3N_4 cantilever could be discriminated from the formed zinc-ordered array on the self-organized ImSi monolayer. The CFM image (Figure 4b) shows the interface of the zinc-array substrate covered with water. Since the observed XPS spectra of ImSi substrate gave the ratio of N to Zn to be around 3, and a parallelogram unit of the zinc-array image was twice as large as that found in the zinc-free ImSi monolayer (Figure 4), each zinc atom may be coordinated to three imidazoline ligands at the ImSi monolayer surface (Scheme 1), and the two-dimensional ordered array of zinc ions was formed at a surface of ImSi substrate (zinc-array substrate).

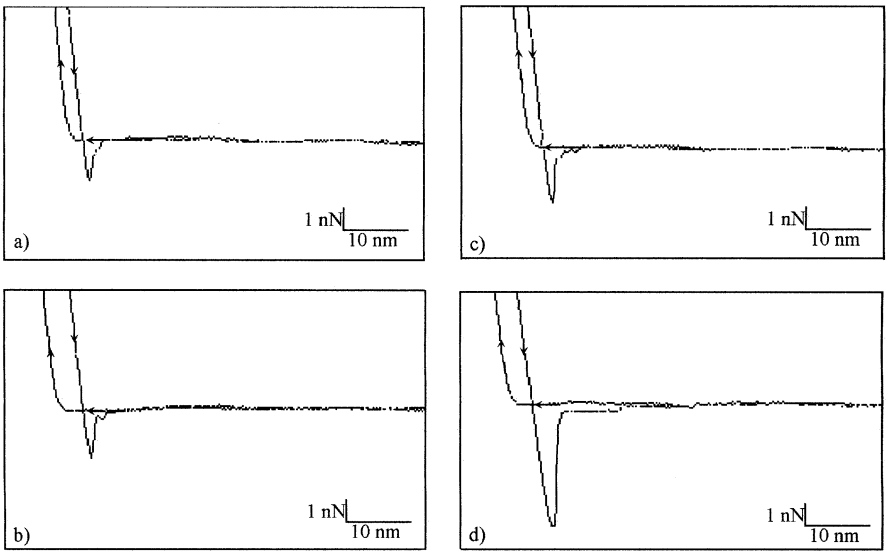

Figure 3. The observed typical force-displacement curves of self-organized ImSi monolayer covered with a) pure water or b) aqueous 5 mM $Zn(NO_3)_2 \cdot 6H_2O$ solution by using an Si_3N_4 cantilever (i.e., AFM) and c) pure water or d) aqueous 5 mM $Zn(NO_3)_2 \cdot 6H_2O$ solution by using an ImSi-modified Si_3N_4 cantilever (i.e., CFM).

Previously we have studied model complexes in which the one water and zinc ion is ligated by three imidazole molecules; these stable zinc complexes were prepared by strong molecular recognition of the designed ligands towards zinc ions in solvent.[8] Since the ImSi molecules have a molecular structure similar to imidazole, some ImSi molecules mounted on the cantilever can ligate a zinc ion (Scheme 2) in a self-organized surface.[10] The adhesion force between the ImSi-modified cantilever and zinc array on ImSi substrate therefore becomes larger (Figure 3).

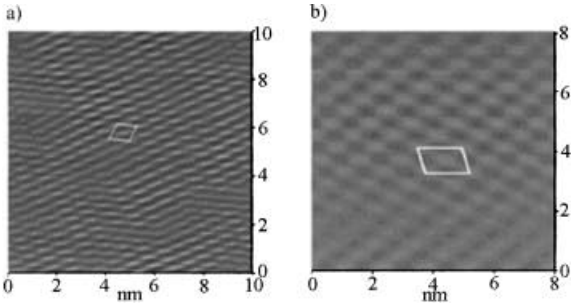

Figure 4. The filtered molecular-resolution CFM image of a) zinc-free ImSi substrate and b) the zinc-array substrate, observed in water. The bright spots/protrusions in the images a) and b) may be attributed to each imidazoline head of ImSi molecules and the zinc ions coordinated by a couple of imidazoline nitrogen atoms, respectively. The parallelograms the images a) and b) indicate the respective units of about 0.9×0.7 nm^2 and about 1.4×0.9 nm^2.

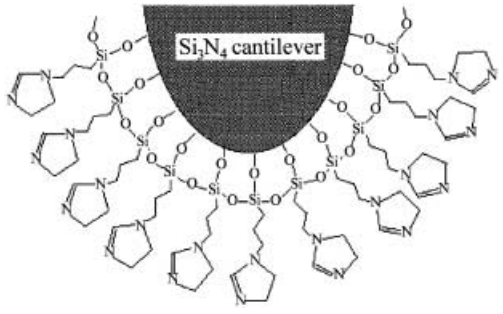

Scheme 2. Schematic diagram of ImSi-modified Si_3N_4 cantilever used in the CFM measurement.

The CA-like activity of the zinc-array substrate, which was estimated by the CO_2–Veronal indicator method[11], generated $\Delta\tau = 0.57$ ($\tau_0 = 67$ s, $\tau = 27$ s) at 0 °C for the pH change

from 8.3 to 7.7. The enzyme conversion rate from CO_2 to HCO_3^- has also been measured for CA and the zinc model compound [Zn(L1S)(OH_2/OH^-)], in which L1S is nitrilotris(2-benzyimidazolylmethyl-6-sulfonate).[8] The aqueous $\sim 0.1\,\mu M$ CA (or $150\,mg\,L^{-1}$) solution gave $\Delta\tau = 0.93$ ($\tau_0 = 15$ s, $\tau = 1$ s) for the pH change of 8.5 to 7.5 at 0 °C.[12] The aqueous $\sim 50\,\mu M$ [Zn(L1S)(OH_2/OH^-)] (or $30\,mg\,L^{-1}$) generated $\Delta\tau$ to be around 0.25 for the change of pH 8.7 to pH 8.0 at 0 °C. The zinc model compound with L1S showed the highest activity among all the other artificial zinc compounds as CA-active sites.[8c, 13] The CA-like activity of the zinc array was higher relative to a solution of [Zn(L1S)(OH_2/OH^-)], and lower than the CA. The zinc array can catalyze the conversion from CO_2 to HCO_3^- and accelerate the calcium carbonate formation.

Biomimetic mineralization: The in vitro biomimetic mineralization by using both zinc-array and chitin substrates prepared by artificial nanotechnique has allowed the formation of calcium carbonate polymorphs in aqueous $10^{-5}/10^{-4}$ % wt pAsp and 10 mM Ca^{+2} solution at pH 9–8, ≤ 25 °C, under a 500–1500 ppm CO_2 atmosphere. After two days, the amount produced was determined; the ΔP values for the zinc-array and zinc-free ImSi substrates were equal to 1.2×10^{-1} and 1.3×10^{-2}, respectively, at 25 °C.[11] The video optical microscopy (VOM) images on the pAsp-coated chitin substrate demonstrated the effect of zinc-array substrate on calcium carbonate morphology (Figure 5). The initially formed film was made up

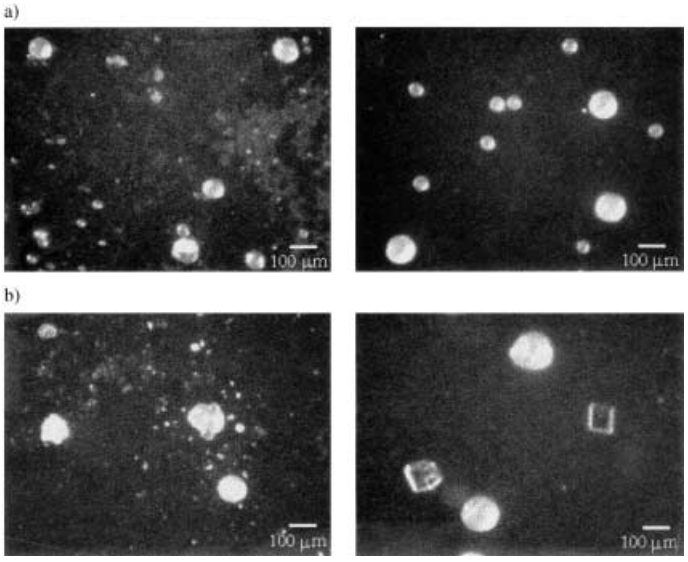

Figure 5. The effect of zinc-array substrate on the crystal morphology formed on pAsp-covered chitin substrate; the VOM images of the formed calcium carbonate on pAsp-covered chitin substrate after calcification for 2 days at 5×10^{-5} % wt pAsp, pH 9.0–8.1, and a) 15 °C or b) 25 °C for the zinc-array substrate (left) and the ImSi substrate free from zinc ions (right).

of many fine particles assembled together in addition to the larger particles with diameters in the 50–120 μm in diameter and was never observed in the presence of zinc-free ImSi substrate.

The observed in-situ X-ray diffraction patterns measured just for the formed calcium carbonate on the substrate demonstrated, for the first time to our knowledge, that the interaction between the zinc-array substrate and the pAsp-coated chitin substrate lead to the efficient formation of vaterite at 25 °C or both calcite and vaterite at 15 °C (Figure 6). On the zinc-free ImSi substrate system, the non-calcite

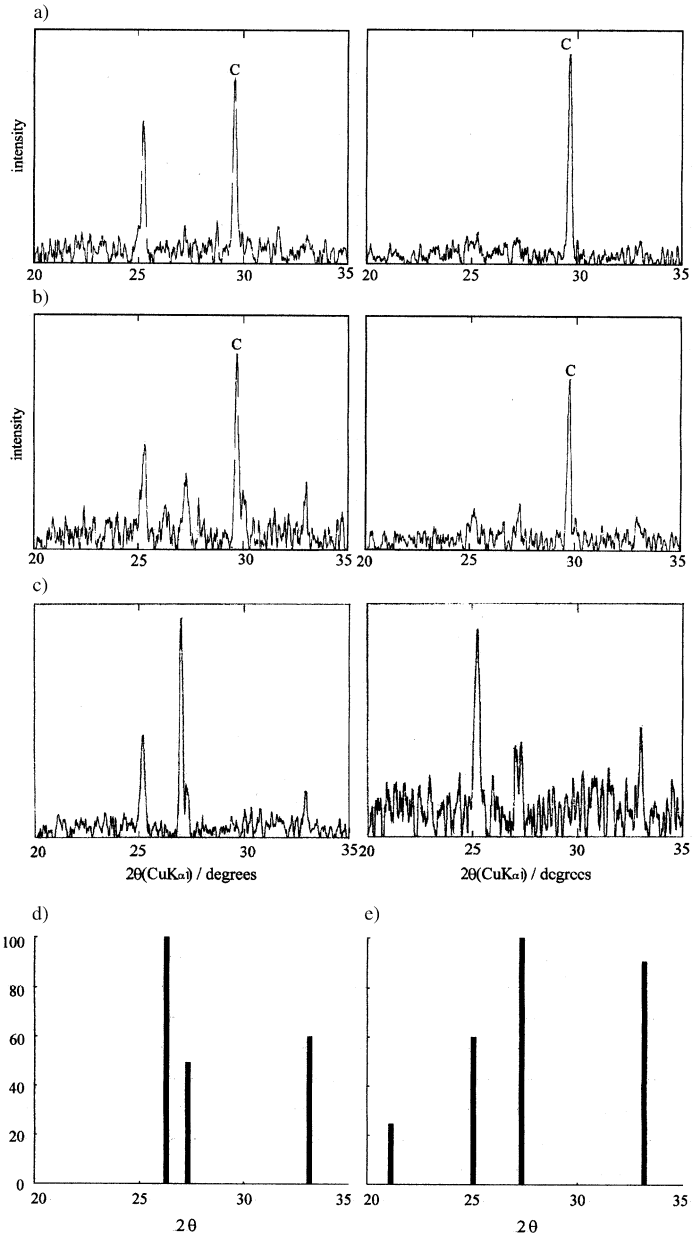

Figure 6. The typical XRD patterns of the formed calcium carbonate on the pAsp-covered chitin substrate after calcification for 2 days in aqueous 5×10^{-5} % wt pAsp solution at a) 15 °C, b) 25 °C, and c) in aqueous 5×10^{-4} % wt pAsp solution at 25 °C, using the zinc-array substrate (left) and the ImSi substrate free from zinc ions (right). The XRD patterns of aragonite and vaterite are shown in d) and e), respectively.

material present only in small quantities deposited on the pAsp-coated chitin substrate (Figure 6). The assignment of the polymorphs to vaterite or calcite was carried out by comparison of the literature data with their XRD patterns (Figure 6d and e).[14] The zinc-array-directing CA activity of the conversion of CO_2 to HCO_3^- leads to the accelerated formation of calcium carbonate polymorphs at a low temper-

ature, 15 °C; the non-calcite never forms in inorganic solution at < 25 °C between pH 7 and pH 9.[15] The calcite component disappears on going from 5×10^{-5} to 5×10^{-4} % wt pAsp at 15 and 25 °C. With increasing pAsp concentration, the amount of calcium carbonate produced decreased for the zinc-free ImSi substrate; the pAsp adsorbed onto the chitin substrate may act as inhibitor against mineralization. The role of the zinc-array substrate is to accelerate CO_2 hydration and calcium carbonate formation within a limited time. The zinc array and pAsp substrates can control the polymorphism and morphology of calcium carbonate (Figures 5–7).

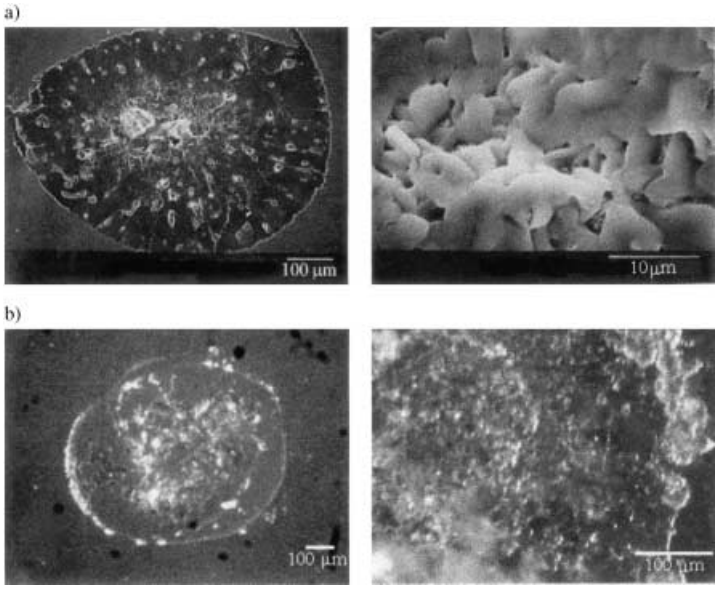

Figure 7. a) SEM image (left) of the formed $CaCO_3$ film on the pAsp-coated chitin substrate in aqueous 5×10^{-4} % wt pAsp solution, associated with SEM image at higher magnification (right). b) VOM images of the formed $CaCO_3$ film on the pAsp-coated chitin substrate in aqueous 5×10^{-4} % wt (left) or 5×10^{-5} % wt (right) pAsp solution. All the images were observed after calcification for 2 days at 25 °C in the presence of the zinc-array substrate.

The observed VOM/SEM images show the $CaCO_3$ film formed on the pAsp-coated chitin substrate in aqueous 5×10^{-4} and 5×10^{-5} % wt pAsp solution at 25 °C after mineralization for 2 days in the presence of the zinc-array substrate (Figure 7). Figure 5b (left) and Figure 7b (right) showed the initial and mature films of calcium carbonate, respectively; these were located at the different portions of a pAsp-coated chitin substrate in aqueous 5×10^{-5} % wt pAsp solution. The Raman bands observed in situ at around 714 and 1084 cm^{-1} were assigned to the symmetric deformation and symmetric stretching vibrations of CO_3^{2-}, respectively.[16] The broad and sharp bands at around 1500 and 3000 cm^{-1} were assigned to the antisymmetric and symmetric stretching vibrations of -COO^- and -CH_2, respectively, arising from pAsp. Thus, the above-mentioned film is an inorganic–organic complex that consists of $CaCO_3$ and pAsp.

Since the chitin substrate was connected to the pAsp coating through hydrogen bonds between the -COO^- groups of pAsp and the amide groups of chitin, the HCO_3^- species can approach each carboxylate-bound Ca^{2+}. The crystal growth of $CaCO_3$ perpendicular to the pAsp-coated chitin substrate was inhibited with increasing pAsp concentration in the absence of the zinc-array substrate, as shown in the right side of Figure 6. Since the nacre of the mollusk shell has a laminated structure that consists of the calcium carbonate and Asp-rich macromolecules, the biomineralization of the mollusk shell was partially reproduced by the in vitro mineralization by using the nanotechniques described in this work.

The biomineralization and biomimetic mineralization reactions may take place as follows: [see Eqs. (1) and (2) below] [17]

$$CO_2 + \text{zinc-bound } H_2O \rightarrow HCO_3^- + H^+ \quad (1)$$

$$HCO_3^- + Ca^{2+} \rightarrow CaCO_3 + H^+ \quad (2)$$

The accumulated protons by biomineralization may be transferred in vivo out of the cell membrane, and the proton concentration within a cell may be kept in physiological condition. The non-calcite formation needs both CA for the conversion from CO_2 to HCO_3^-, and chitin substrate-adsorbed pAsp for the recognition sites of the calcium ions. The CA-accerelated calcium carbonate formation and the promoted polymorphs may be indispensable for the well-being of marine invertebrate animals. The non-calcite is never deposited from inorganic solution, which consists of both Ca^{2+} and HCO_3^- at about pH 7–8.5 at ≤ 25 °C[15] by a chemical reaction associated with the evolution of carbon dioxide as follows [Eq. (3)]:

$$2HCO_3^- + Ca^{2+} \rightarrow CaCO_3 \text{ calcite} + CO_2 \uparrow + H_2O \quad (3)$$

Experimental Section

Materials: 3-(2-Imidazolin-1-yl)propyltriethoxysilane (ImSi) was obtained from Fluka, poly(*L*-asparate) (pAsp) from Sigma, chitin from Seikagaku Kogyo, and $Zn(NO_3)_2 \cdot 6H_2O$, $Ca(NO_3)_2 \cdot 4H_2O$ and $(NH_4)_2CO_3$ from Wako. These commercial reagents were used as obtained without further purification.

Preparation of the ImSi-coated mica substrate (ImSi substrate): Freshly stripped mica (Nisshin EM) was immersed in a solution of 10 v/v % sodium methoxide in methanol at 50 °C for 1 min. Then ImSi molecules were adsorbed on the mica surface by immersing the mica solution of ImSi (~1 mM)in *n*-hexane for 2 h under a nitrogen atmosphere.[9]

Preparation of zinc ordered array onto ImSi substrate (zinc-array substrate): The zinc array substrate was prepared by immersing the ImSi substrate into aqueous solution of 5 mM $Zn(NO_3)$ at about pH 8.5.

Preparation of chitin-coated glass substrate (chitin substrate): The chitin substrate was prepared by immersing a strip of cover glass into a solution of *N*,*N*-dimethyl-acetamide and *N*-methyl-2-pyrrolidone (50/50 : w/w) containing 0.4 % wt chitin.[19] The chitin substrate was covered with pAsp, which has many carboxylate groups as calcium-binding sites.

Determination of the CA-like activity ΔT of zinc-array substrate: The CA-like activity $\Delta\tau$ for zinc-array substrate was determined by using the CO_2–Veronal indicator method.[11, 12] $\Delta\tau$ was defined as $(\tau_0 - \tau)/\tau_0$ to give a numerical value for the enzymatic activity of CO_2 hydration of the zinc-array substrate; τ or τ_0 was the time interval required for the pH change in the presence or absence of zinc, respectively.

Calcium carbonate formation reaction: The calcification reaction, the container of which is shown Figure 8, was carried out for 2 days in a solution of $Ca(NO_3)_2 \cdot 4H_2O$ (10 mM) associated with the zinc-array and

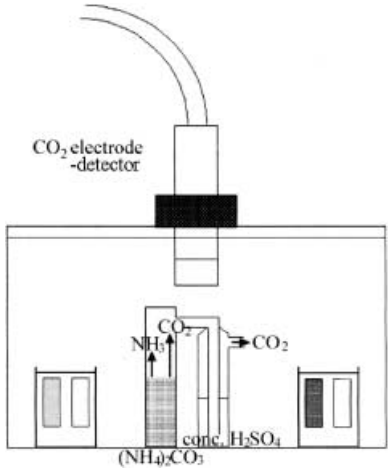

Figure 8. The apparatus for calcium carbonate formation reaction. An pAsp-coated chitin substrate (open rectangle), zinc-free ImSi substrate (gray rectangle), and zinc array substrate (dark rectangle) are immersed into aqueous 10 mM $Ca(NO_3)_2 \cdot 4H_2O$ and $5 \times 10^{-5}/5 \times 10^{-4}$ % wt pAsp solution.

chitin substrates, covered with $10^{-5}/10^{-4}$ % wt pAsp, under a CO_2 atmosphere of 0.05 – 0.15 % v/v at 15 or 25 °C and pH 9 – 8. The pH was adjusted to 9.0 by using AMPSO buffer, and just before starting the calcification decreased to about pH 8 and remained at this pH over 2 days. The CO_2 concentration in the atmosphere of a closed reaction-container was monitored by a CO_2 detector-CGDIC-7 (TOA); CO_2 was supplied by the decomposition of $(NH_4)_2CO_3$, and the other decomposed component NH_3 was eliminated by concentrated H_2SO_4. If NH_3 was not eliminated, the pH of the reaction solution increased from pH 9.0 to about 9.5, and the calcium carbonate polymorphism was further accelerated. The marine invertebrate animals may be kept at a pH of no more than 8.5. The reaction container was put into an incubator-LNC-111 (TABAI) at 15 or 25 °C.

Determination of the amount of calcium carbonate produced (ΔP): The ΔP value was estimated from $(P_0 - P)/P_0$; P and P_0 is the concentration of the calcium ion (mg L^{-1}) in aqueous solution after the calcium carbonate formation reaction in two days and its initial concentration, respectively.[12] The calcium concentration in aqueous solution was determined by using atomic absorption spectrometry.

Atomic force microscopy (AFM): All the AFM images were measured in the constant-force mode.[20] The sample surface was imaged by mechanically tracing its topography by means of a microfabricated cantilever with an integrated pyramidal Si_3N_4 tip. Here, the cantilever's force constant was $k = 0.58$ N m^{-1}. In our experiments the scanning force over the substrate surface was $F = 10 - 20$ nN in air and $F = 1 - 2$ nN in water; the image acquisition time was less than 10 s.

Chemical force microscopy (CFM): The chemical force microscope[21] images identifying the zinc array were measured by using a Nano Scope III (DI) and ImSi-modified Si_3N_4 cantilever (Scheme 2), which was prepared as follows. The tips of Si_3N_4 cantilever were covered with a solution of concentrated H_2SO_4 and 30 % H_2O_2 (70:30 v/v), and heated at 70 °C for 30 min.[9b, 22] They were immediately rinsed by completely covering them with distilled water and decanting the liquid; the process was repeated at least three times. They were stored in water until used. The ImSi molecules were adsorbed on the modified and cleaned cantilevers, and immersed into a solution of ImSi (~1 mM) in *n*-hexane for 1 h under a nitrogen atmosphere.[9b, 22] The angle-dependent XPS survey spectra of ImSi adsorbed onto Si_3N_4 substrate showed that the intensity of the carbon signal was increased relative to that of silicon and oxygen signals as with the angle between a plane of an electron detector and the normal line to a surface (takeoff angle) decreased. These results demonstrate a monolayer model as a hydrocarbon layer adsorbed onto Si_3N_4 cantilever.[22]

In AFM or CFM measurements a stainless-steel cup, on which the zinc-array and ImSi substrate were mounted, was sealed by a O-ring against a glass cell filled with the aqueous solution.[23] In order to make clear that the ImSi-modified Si_3N_4 cantilever selectively recognized the zinc ions, the force-displacement curves were measured a minimum of one hundred times for ten portions of each surface of the ImSi and zinc-array substrates. The adhesion force, which was defined as the difference between a minimal force and a nontouching line as the pull-out force in these curves,[24] was determined from the observed force-displacement curves.

X-ray photoelectron spectroscopy (XPS): The zinc array substrate was confirmed by XPS measurements; the XPS spectra were acquired on a XPS-700 (RIGAKU) instrument.

Video optical microscopy (VOM) and scanning electron microscopy (SEM): The calcium carbonate polymorphs/films formed on the pAsp substrate were observed in situ by using OVM-7310 (CHROMA) in combination with 200 × and 650 × magnification lenses; they were also analyzed at higher magnification by using an SEM-2100A (HITACHI) instrument.

X-ray diffractiometry (XRD): The calcium carbonate polymorphs formed on the pAsp substrate were analyzed by using XRD. The X-ray diffraction patterns were acquired on a XRD-MiniFlex (RIGAKU) diffractometer.

Raman spectroscopy: The $CaCO_3$ films grown on pAsp-coated chitin substrate were analyzed by using Raman spectroscopy. The Raman spectra were acquired on a RAMANOR-T64000 (JOBINYVON) instrument.

Acknowledgement

NS thanks Dr. M. M. Ibrahim for his discussion in the early work.

[1] a) S. Weiner, W. Traub, *Philos. Trans. R. Soc. London Ser. B* **1984**, *304*, 425; b) L. Addadi, S. Weiner, *Proc. Natl. Acad. Sci.*, **1985**, *82*, 4110; c) L. Addadi, S. Weiner, *Angew. Chem.* **1992**, *104*, 159; *Angew. Chem. Int. Ed. Engl.* **1992**, *31*, 153; d) S. Weiner, L. Addadi, *J. Mater. Chem.* **1997**, *7*, 689; e) Y. Levi, S. Albeck, A. Brack, S. Weiner, L. Addadi, *Chem. Eur. J.* **1998**, *4*, 389.

[2] S. Mann in *Biomineralization: Chemical and Biochemical Perspectives* (Eds.: S. Mann, J. Webb, J. P. Williams), Wiley-VCH, New York, **1989**, p. 35.

[3] H. Miyamoto, T. Miyashita, M. Okushima, S. Nakano, T. Morita, A. Matsushiro, *Proc. Natl. Acad. Sci.* **1996**, *93*, 9657.

[4] a) T. Samata, N. Hayashi, M. Kono, K. Hasegawa, C. Horita, S. Akera, *FEBS Lett.* **1999**, *462*, 225; b) M. Kono, N. Hayashi, T. Samata, *Biochem. Biophys. Res. Commun.* **2000**, *269*, 213.

[5] J. Aizenberg, J. Kanson, T. F. Koetzle, S. Weiner, L. Addadi, *J. Am. Chem. Soc.* **1997**, *119*, 881.

[6] A. M. Belcher, X. H. Wu, R. J. Christense, P. K. Hansma, G. D. Stucky, D. E. Morse, *Nature* **1996**, *381*, 56.

[7] T. F. Goreau, *Biol. Bull.* **1959**, *116*, 59.

[8] a) K. Ichikawa, K. Nakata, M. M. Ibrahim, *Chem. Lett.* **2000**, 296; b) K. Nakata, N. Shimomura, N. Shiina, M. Izumi, K. Ichikawa, M. Shiro, *J. Inorg. Biochem.* **2002**, *89*, 225; c) K. Nakata, M. K. Uddin, K. Ogawa, K. Ichikawa, *Chem. Lett.* **1997**, 991.

[9] a) T. Nakagawa, K. Ogawa, Kurumizawa, *Langmuir* **1994**, *10*, 525; b) A. Ulman in *Ultrathin Organic Films*, Academic Press, New York, **1991**.

[10] a) K. Nakata, S. Kawabata, K. Ichikawa, *Acta Crystallogr. Sect C.* **1995**, 1092; b) K. Ichikawa, M. Khabir Uddin, K. Nakata, *Chem. Lett.* **1999**, 115.

[11] S. Y. Yang, M. Tsuzuki, S. Miyauchi, *Plant Cell Physiol.* **1985**, *26*, 25.

[12] N. Shimomura, N. Ohkubo, K. Ichikawa, Chem. Lett. **2002**, 902

[13] a) P. Woolly, *Nature* **1975**, *258*, 677; b) R. S. Brown, N. J. Curtis, J. Huguet, *J. Am. Chem. Soc.* **1981**, *103*, 6953; c) R. S. Brown, D. Salmon, N. J. Curtis, S. Kusuma, *J. Am. Chem. Soc.* **1982**, *104*, 3188; d) H. Slebocka-Tilk, J. L. Concho, Z. Frakman, R. S. Brown, *J. Am. Chem. Soc.* **1984**, 106, 2421; e) X. Zhang, R. van Eldik, T. Koike, E. Kimura, *Inorg. Chem.* **1993**, *32*, 5749; f) X. Zhang, R. van Eldik, *Inorg. Chem.* **1995**, *34* 5606.

[14] a) P. Swarthmore in *Powder Diffraction File Set 33*, International Centre for Diffraction Data, Pennsylvania, **1989**; b) P. Swarthmore in *Powder Diffraction File Set 41,* International Centre for Diffraction Data, Pennsylvania, **1991**.

[15] Y. Kitano, *Bull. Chem. Soc. Jpn.* **1962**, *35*, 1980.
[16] a) K. Nakamoto in *Infrared and Raman Spectra of Inorganic and Coordinated Compounds*, 3rd ed., Wiley-VCH, New York, **1978**; b) L. Wang, I. Sondi, E. Matijevic, *J. Colloid Interface Sci.* **1999**, *218*, 545.
[17] a) A. P. Wheeler, J. W. George, C. A. Evans, *Science* **1981**, *212*, 1397; b) A. H. Borman, E. W. Jong, M. Huzinga, D. J. Kok, P. Westbroek, L.Bosch, *Eur. J. Biochem.*, **1982**, *129*, 179.
[18] J. Sagiv, *Isr. J. Chem.*, **1979**, *18*, 339.
[19] T. Kato, T. Suzuki, T. Irie, *Chem. Lett.* **2000**, 186.
[20] G. Binning, C. F. Quate, C. Gerber, *Phys. Rev. Lett.* **1986**, *56*, 930.
[21] a) J. N. Israelachvili in *Intermolecular and Surface Forces*, Academic Press, New York, **1992**; b) T. Nakagawa, K. Ogawa, T. Krumizawa, S. Ozaki, *Jpn. J. Appl. Phys.* **1993**, *32*, L294; c) C. D. Frisble, L. F. Rozsnyai, A. Noy, M. S. Wrighton, C. M. Liever, *Science* **1994**, *265*, 2071.
[22] a) T. Ito, M. Namba, P. Buhlmam and Y. Umezawa, *Langmuir*, **1997**, 13, 4323; b) V. V. Tsukruk, V. N. Bliznyuk, *Langmuir*, **1998**, 14, 446; c) Stephen R. Wasserman, Yu-Tai Tao, George M. Whitesides, *Langmuir* **1989**, *5*, 1074.
[23] K. Ichikawa, M. Yamada, *J. Phys. Condens Matter* **1996**, *8*, 4889.
[24] a) A. L. Weisenhorn, P. Maivald, H.-J. Butt, P. K. Hansma, *Phys. Rev. B* **1992**, *45*, 11226; b) J. H. Hoh, J. -P. Revel, P. K. Hansma, *Nanotechnology*, **1991**, *2*, 119.

Received: October 28, 2002 [F4534]

